Journal for Technology and Science
Homepage : https://journal.antispublisher.com/index.php/IPTEKS/index
Email : admin@antispublisher.com

e-ISSN : 3047-4337
JOTECH, Vol. 3, No. 4, October 2026
Page 177-196

Alkali-Metal Gated Valence Tautomerism in a Crown Ether Appended Cobalt–Dioxolene Complex

Ragheed Raad Faisal
General Directorate of Education Nineveh, Mosul, Iraq

DOI : https://doi.org/10.61796/ipteks.v3i4.614

Sections Info

Article history:
Submitted: June 23, 2026
Final Revised: July 11, 2026
Accepted: August 16, 2026
Published: September 12, 2026

Keywords:
Valence tautomerism
Cobalt–dioxolene
Crown ether
Host–guest recognition
molecular switch
intramolecular electron transfer
supramolecular electrostatic gating
Redox-active ligand

ABSTRACT

Objective: *Controlling intramolecular metal–ligand electron transfer with a chemically addressable, non-invasive input remains a central objective in the design of molecular electronic switches.* ***Method:*** *Here we report a crown-ether-appended cobalt–dioxolene complex, [Co(bpy-B18C6)(3,5-dbdiox)2] (1), in which a benzo-18-crown-6 receptor is tethered to a bipyridine ancillary ligand and positioned peripheral to the redox-active {Co(dioxolene)2} core. Recognition of alkali-metal cations (Li+, Na+, K+, Rb+, Cs+) at the remote crown ether, quantified by UV–Vis–NIR titration (K+: log Ka = 4.72 in CH2Cl2), reversibly biases this equilibrium toward the ls-Co(III)–cat state without the cation coordinating to cobalt. A crown-free control complex is essentially unresponsive to added cations, and broken-symmetry DFT reproduces the selective electrostatic stabilisation of the catecholate manifold. Sequestration of the bound cation with cryptand [2.2.2] restores the initial state, delivering a reversible supramolecular switch that retains ≥95% of its amplitude over six cycles.* ***Results:*** *The complex exhibits thermally accessible valence tautomerism between a low-spin Co(III)–catecholate (ls-Co(III)–cat) state and a high-spin Co(II)–semiquinonate (hs-Co(II)–SQ) state. Cation binding raises the valence-tautomeric transition temperature by up to 48 K, shifts the dioxolene-centred redox couple anodically by up to 86 mV, contracts the mean Co–O and Co–N bonds by ca. 0.12 and 0.17 Å, and lowers the room-temperature magnetic moment. The magnitude of the electronic perturbation tracks recognition strength but deviates measurably for the largest cation, indicating that the through-space charge–core distance, not binding affinity alone, governs the response.* ***Novelty:*** *The results establish alkali-metal recognition as a remote electrostatic gate for valence tautomerism.*

INTRODUCTION

The molecules that can be switched between two or more different electronic structures with an external stimulus are essential to molecular-electronic, information storage, sensing, and responsive materials [1, 2]. Reversible molecular switching is particularly interesting, since the oxidation state, spin, colour, molecular geometry and magnetic moment can all be different in the two conformations of the molecule [2,3]. This behavior is endowed to a natural platform through the use of redox active ("non-innocent") ligands, which bring the energies of ligand and metal based frontier orbitals close together and thus allow for exchange of charge between the two [3]. When there are redox isomers that are sufficiently close in free energy to each other to be able to convert between them with a mild stimulus, this is called valence tautomerism (VT). In spin-crossover, the metal oxidation state remains unchanged, whereas in VT the spin change is the result of an electron transfer that involves the change of formal oxidation state [4, 5].

The archetypal VT systems are the cobalt complexes with the o-dioxolene ligands that have two redox states: catecholate (cat, dianionic) and semiquinonate (SQ, radical monoanionic) [6, 7, 8]. The latter complexes exhibit an intramolecular equilibrium of the

type ls-Co(III)–cat ⇌ hs-Co(II)–SQ, where intramolecular electron transfer from the catecholate to the metal changes the low-spin Co(III) (d^6, S = 0) into high-spin Co(II) (d^7, S = 3/2) and the donor ligand from Co(III) to Co(II) is oxidised [6, 9]. These signatures enable the two electromers to be distinguished by structural, spectroscopic and magnetic measurements [6, 8, 9] and the transition features a change in metal oxidation state, a change in ligand oxidation state, a change in overall spin, a pronounced contraction or elongation of the Co–O and Co–N bonds. The difference in free energy between the two electromers is expected to be close to the thermal energy at the temperature of interest, so that it is possible to observe a transition [9] [10] [11] which is entropy-driven toward the high-spin, high-volume hs-Co(II)–SQ form. In particular, this free-energy difference has been found to be related to the difference in the metal- and ligand-centred redox potentials, giving rational, electrochemical control of the transition [10], [17].

Physical stimuli are the stimuli conventionally used to drive VT. Thermal control is ubiquitous, and systems based on cobalt–tetraoxolene and cobalt–dioxolene have hysteretic transitions near room temperature that are well known [12]. Molecular solids and switchable frameworks can also be populated with metastable VT states by photoexcitation; however, in many cases the photoinduced state is transient and only exists at cryogenic temperatures [13], [14], [15], [35]. The balance between the two electromers is influenced by the pressure, the polarity of the solvent, lattice solvation and the electronic nature of the ancillary ligand and contemporary research has been focused on the prediction and design of the transition by a judicious design of the ligand and environment [2, 16, 17]. The control of VT by chemically-programmable molecular-recognition events as opposed to bulk physical parameters is comparatively underdeveloped.

The prototype synthetic receptors of alkali-metal cations are the crown ethers which exhibit a selective binding by the perfect size of the cavity and the radius of the cation: 18-membered macrocycles like 18-crown-6 are the optimal receptors for K+ [18], [19], [20], [22]. The introduction of a localised positive charge from host–guest capture of a cation can in principle act as an electrostatic influence to a neighbouring redox-active centre. This is the principle of operation of redox-active ionophores, which involve a shift in the formal potential of an appended reporter (classically a ferrocene) brought about by the binding of a cation at a receptor, the extent of which depends on the charge-to-size ratio of the binding guest and its distance from the redox unit, either due to space effects or due to conformational changes [23]. The conceptual advance here is to enable the simultaneous binding of both of these two well-developed but largely independent areas: the occupancy of the crown ether changes the local electrostatic environment of the cobalt–dioxolene unit and thus its electron-transfer energetics [21, 23].

Research gap

This study is motivated by three gaps. Cobalt–dioxolene VT is a field that is well understood but the vast majority of switching demonstrations use a temperature, light or pressure input, and very few use molecular recognition [9], [10]. Second, the two processes, namely, host–guest chemistry and valence tautomerism have been developed to a high degree of sophistication, but a strategy of deliberately coupling a peripheral crown ether for the recognition of alkali metals with a metal–ligand electron transfer process in a cobalt–dioxolene core which one never actually encounters, has not been

developed as a general control strategy [23]. Third and most important: A convincing demonstration should not only report that a spectrum changes when a salt is added, but it must also be able to explain the changes. The mechanism that is required is given as: Alkali-Metal binding, Local electrostatic and structural perturbation, Change in the Co/dioxolene redox energetics, Redistribution of the valence tautomers, Reversible electronic switching. The key scientific question that is discussed below is establishing that cause and effect relationship, and identifying the specific effect of the crown compared to the effect of ionic strength or counter-anion.

Aim, hypothesis and contribution

The overall objective of this research is to see if the electron transfer and valence tautomerism between a cobalt center and a dioxolene ligand in a pendant crown-ether receptor is reversibly controlled by binding to the alkali metals. We hypothesize that binding of an alkali-metal cation within the appended crown ether will cause a local electrostatic perturbation that will alter the relative energies of the Co(III)–catecholate and Co(II)–semiquinonate manifolds, favoring the more negatively charged catecholate manifold, which in turn will shift the valence-tautomeric equilibrium; upon release of the cation, the original equilibrium will be restored, creating a reversible supramolecular electronic switch. To test this we designed a complex where the recognition site is placed peripheral but electrostatically close to the redox active core, and we interrogate the response using a converging set of tools: host–guest titration, variable-temperature UV–Vis–NIR and magnetometry, EPR, electrochemistry, single-crystal X-ray diffraction, reversibility cycling and broken-symmetry DFT.

The contribution we ascribe is not the synthesis of a new cobalt complex itself, but the introduction of cation recognition as a 'chemically addressable' supramolecular 'gate' for intramolecular metal–ligand electron transfer in a valence-tautomeric system. In particular, it shows that the two types of recognition, host–guest and redox-active coordination chemistry, are coupled in a single molecule, that a binding event can be translated into a measurable electronic-state change, that a cation dependent modulation of the VT equilibrium is identified, that the strength of the recognition could be correlated quantitatively with the degree of electronic perturbation, that switching is reversible over multiple cycles, and that the influence of the remote binding of a closed-shell ion on electron transfer is rationalized both experimentally and theoretically. This is not a synthetic novelty but the intended advance and mechanistic depth.

METHODOLOGY

Materials and general procedures

The reduced ls-Co(III)–cat form is air-sensitive, and all the manipulations of the cobalt complexes were done under dry, oxygen-free dinitrogen using the standard Schlenk techniques and a glovebox. Solvents were dried over activated alumina and degassed by three freeze–pump–thaw cycles before use, while dichloromethane for spectroscopy and electrochemistry was also dried over 4 Å molecular sieves and the amount of water detected by Karl-Fischer titration (<15 ppm). The 3,5-di-tert-butylcatechol and the cobalt(II) acetate tetrahydrate were commercially available.Co(II) acetate tetrahydrate and the bipyridine precursors were available commercially. The common weakly coordinating counter-anion, tetrakis[3,5-

bis(trifluoromethyl)phenyl]borate (BArF4–) was used for all alkali-metal cations, by preparing M[BArF4] (M = Li, Na, K, Rb, Cs) from these salts and drying them rigorously before use, eliminating the need to introduce the counter-anion as an additional variable across the alkali-metal series. Full synthetic procedures and characterisation is provided in Appendix A.

Instrumentation and physical measurements

The 1H/13C NMR and HRMS were used to characterize the ligands, while HRMS, elemental analysis, FTIR, UV–Vis–NIR, EPR, electrochemistry, variable-temperature magnetometry and single-crystal X-ray diffraction were employed to characterize the paramagnetic complexes. The assignments of diagnostic ν(C–O) stretches of catecholate and semiquinonate were made by FTIR spectra. UV–Vis–NIR spectra were measured from 300 to 3000 nm and EPR spectra were measured at X-band on frozen solutions. Cyclic and differential-pulse voltammetry were conducted in CH2Cl2 in the presence of 0.1 M [NBu4][BArF4] as the supporting electrolyte, and using the ferrocenium/ferrocene (Fc+/Fc) couple as the reference. The susceptibility measurements were performed on a SQUID magnetometer in the range of 2- 400K. Conditions for the observations and the technique used are summarized in Table 1, but not spread throughout the text.

Table 1. Experimental techniques and the conditions under which cation binding and valence tautomerism were probed.

Technique	Information obtained	Sample / solvent	Temperature	Key conditions
UV–Vis–NIR	VT populations; binding isotherms	CH_2Cl_2, 10^{-4}–10^{-3} M	233–380 K	300–3000 nm; 1 cm cell
EPR (X-band)	radical (SQ) vs hs-Co(II) response	frozen CH_2Cl_2	100–298 K	9.4 GHz; 1 mW
CV / DPV	metal- and ligand-centred potentials	CH_2Cl_2	298 K	0.1 M $[NBu_4][BArF_4]$; vs Fc^+/Fc
SQUID	χMT; VT fraction vs T	microcrystalline	2–400 K	0.1 T
SC-XRD	bond metrics; cation site	single crystal	150, 298 K	Mo Kα
FTIR	ν(C–O) cat vs SQ markers	ATR, solid	298 K	400–4000 cm^{-1}
HRMS / EA	composition; stoichiometry		298 K	ESI(+)
DFT (BS)	state energies; spin/charge	gas + CPCM	0 K (electronic)	B3LYP-D3/def2-TZVP

Synthesis of the crown-appended ligand and complexes

To capture a cation above and electrostatically close to the plane of the {Co(dioxolene)2} core, the ancillary ligand bpy-B18C6, a 2,2′-bipyridine with a benzo-18-crown-6 unit attached at the 4-position through a short ether linker, was prepared.

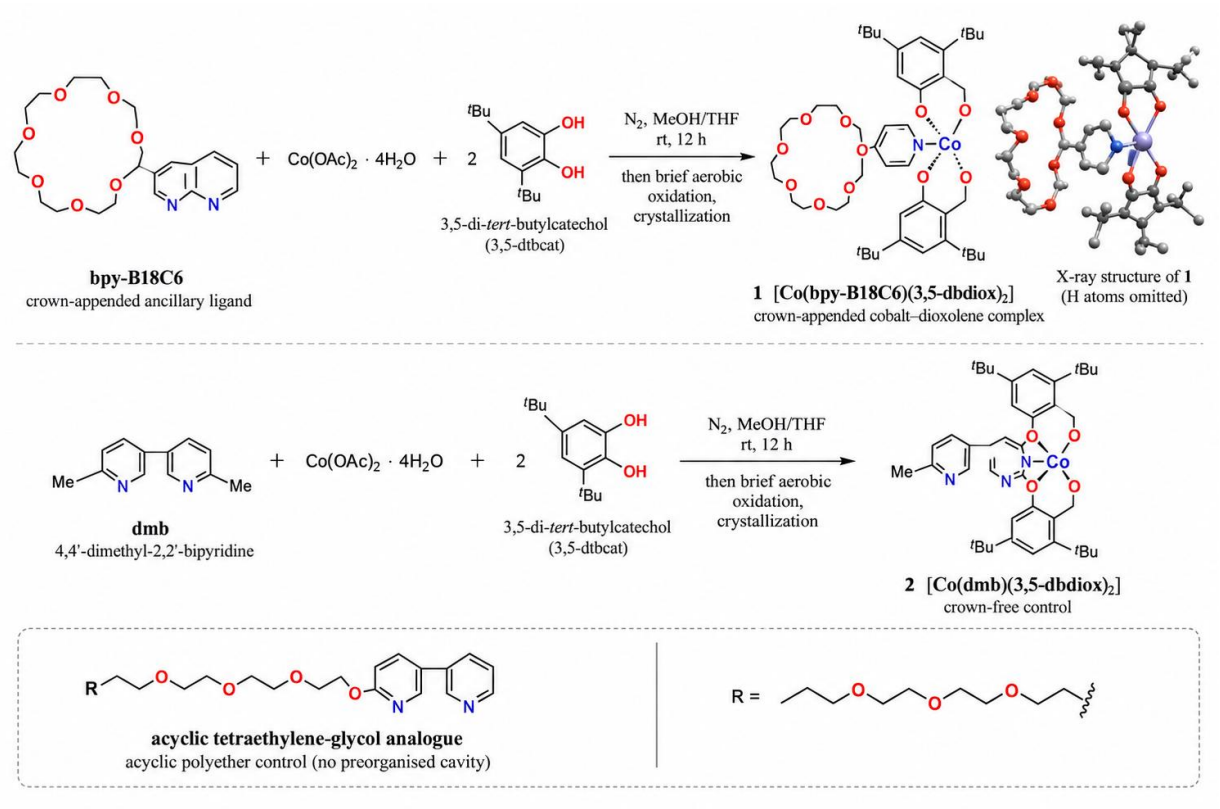

Scheme 1. Molecular structures and synthesis of the crown-appended cobalt–dioxolene switch. The crown-appended ligand bpy-B18C6 is used to prepare complex 1; crown-free complex 2 and the acyclic tetraethylene-glycol analogue are shown as control architectures.

In order to introduce the mixed cat/SQ redox level into the complex [Co(bpy-B18C6)]2+ (1) was assembled using Co(II) acetate, 3,5-di-tert-butylcatechol and bpy-B18C6 under an inert atmosphere with the brief aerobic oxidation and subsequent crystallization. A sterically and electronically similar but crown-free control complex, [Co(dmb)(3,5-dbdiox)2] (2) (dmb = 4,4′-dimethyl-2,2′-bipyridine), was synthesized similarly to allow conclusions regarding the necessity of the crown for an electronic response to the addition of cations. The structure of an acyclic tetraethylene-glycol analogue (no preorganised cavity) is prepared in Appendix A (see below) and detailed procedures, yields and characterisation data (NMR of precursors; HRMS, EA, FTIR of 1 and 2) are provided.

Alkali-metal binding experiments

The binding of Li+, Na+, K+, Rb+ and Cs+ (as BArF4– salts) to 1 in CH2Cl2 was quantitatively measured using a titration method that follows the diagnostic near-IR band of the ls-Co(III)–cat (see Section 3). Job-plot analysis of the absorbance was performed to provide supporting information for the determination of the stoichiometry, but was not the basis for the determination of the association constant [24]. The salts, anion, ranges of solvent and concentration and temperatures employed are listed in Table 2. In the electronic state that was allowed, a cross check by ESI-MS and by ^{1}H NMR of the diamagnetic ligand region was performed.

Table 2. Alkali-metal salts and conditions used for the host–guest binding studies (host 1 at 1.0×10^{-4} M).

Cation	Salt	Anion	Solvent	$[M^+]$ range	Temp.
Li^+	$Li[BArF_4]$	$BArF_4^-$	CH_2Cl_2	0–2.0 mM (0–20 eq.)	298 K
Na^+	$Na[BArF_4]$	$BArF_4^-$	CH_2Cl_2	0–2.0 mM (0–20 eq.)	298 K
K^+	$K[BArF_4]$	$BArF_4^-$	CH_2Cl_2	0–2.0 mM (0–20 eq.)	298 K
Rb^+	$Rb[BArF_4]$	$BArF_4^-$	CH_2Cl_2	0–2.0 mM (0–20 eq.)	298 K
Cs^+	$Cs[BArF_4]$	$BArF_4^-$	CH_2Cl_2	0–2.0 mM (0–20 eq.)	298 K

Spectroscopic, magnetic, electrochemical and structural probes of VT

The influence of cation binding on the electronic state was evaluated in the free complex and in each of the cation bound forms. Also, UV–Vis–NIR spectroscopy provides information about the ligand-centred and charge transfer bands that are characteristic of the ls-Co(III)–cat configuration versus the hs-Co(II)–SQ configuration, while EPR will distinguish the narrow high-spin Co(II) response from the S = 1/2 semiquinonate radical of the ls-Co(III)–cat configuration. The VT fraction as a function of temperature was obtained by variable-temperature UV–Vis–NIR and the thermodynamic parameters ΔH°VT and ΔS°VT were determined. Direct energetic connection between recognition and electron transfer was established by electrochemistry methods (CV and DPV) which were used to identify the location of the ligand and metal-centered redox couples, as well as to determine the metal binding-induced shift in their potentials. To correlate the electronic change with bond-length changes, and to place the trapped cation with respect to the redox core, both single-crystal X-ray structures of the unbound complex and of the K+-bound complex were determined.

Reversibility experiments

The entire cycle from 1 to +M+ to [1⊃M]+ to cation removal and back to 1 was repeated as the central claim in the paper was reversible switching. The guest was removed using cryptand[2.2.2] (4,7,13,16,21,24-hexaoxa-1,10-diazabicyclo[8.8.8]hexacosane), a high-affinity alkali-metal sequestering ligand [21, 25]. The switching amplitude and the percentage signal retention were calculated after each half-cycle and the ls-Co(III)–cat marker band was re-measured.

Computational details

The electronic structures of the free and K+-bound complexes were evaluated computationally using the ORCA program [26] within density functional theory. The geometries and energies were calculated at B3LYP level [27, 28] using the def2-TZVP basis set [29] and Grimme's dispersion correction D3 [30] and within the broken-symmetry formalism [31] the high-spin, open-shell hs-Co(II)–SQ state was described, as

well as the ls-Co(III)–cat state, with solvation treated by the conductor-like polarizable continuum model (CPCM) for dichloromethane [32]. This trapped cation was explicitly placed into the crown ether. For each state, relative electronic energies, spin densities, atomic charges, optimized bond lengths, frontier orbital energies and electrostatic potential maps were calculated, as in previously examined magnetically bistable cobalt systems [33]. Full computational specifications are given in Appendix A.

Data analysis

All titration and variable temperature measurements were repeated three times. Values for association constants and thermodynamic parameters are presented as mean values with standard deviations propagated from non-linear fits [24]. The two electromers gave populations using the calibrated intensity of the ls-Co(III)–cat marker band which were consistent within the quoted limits of error when cross-checked with χMT. The reported quantities are the mean values of the replicates.

RESULTS AND DISCUSSION

Results

Molecular design, synthesis and baseline electronic structure

In the design, the recognition site is designed to be located where a cation captured can have a through-space electrostatic effect to the redox core, but is not formally coordinated to cobalt (Fig. 1). The benzo-18-crown-6 unit is attached to the 4-position of one pyridine ring of the ancillary bipyridine in such a way that, after cation capture, the positive charge is above the {Co(dioxolene)2} plane with a through-space Co···M distance of ca. 8 Å (Section 3.7). Air sensitive, crystalline, Complex 1 was isolated and formulated using HRMS and elemental analysis (Appendix A). The near-IR region of the spectrum exhibits an intense band at 2500 nm that is only observed when cat and SQ are present together (i.e. the ls-Co(III) electromer). The FTIR spectrum exhibits both the features of the catecholate and the features of the semiquinonate, and the EPR spectrum displays a narrow signal at $g \approx 2.004$ characteristic of a semiquinonate in the low-spin form. This band is hence used as the quantitative indicator throughout for the ls-Co(III)–cat population. Baseline parameters are obtained in Table 3.

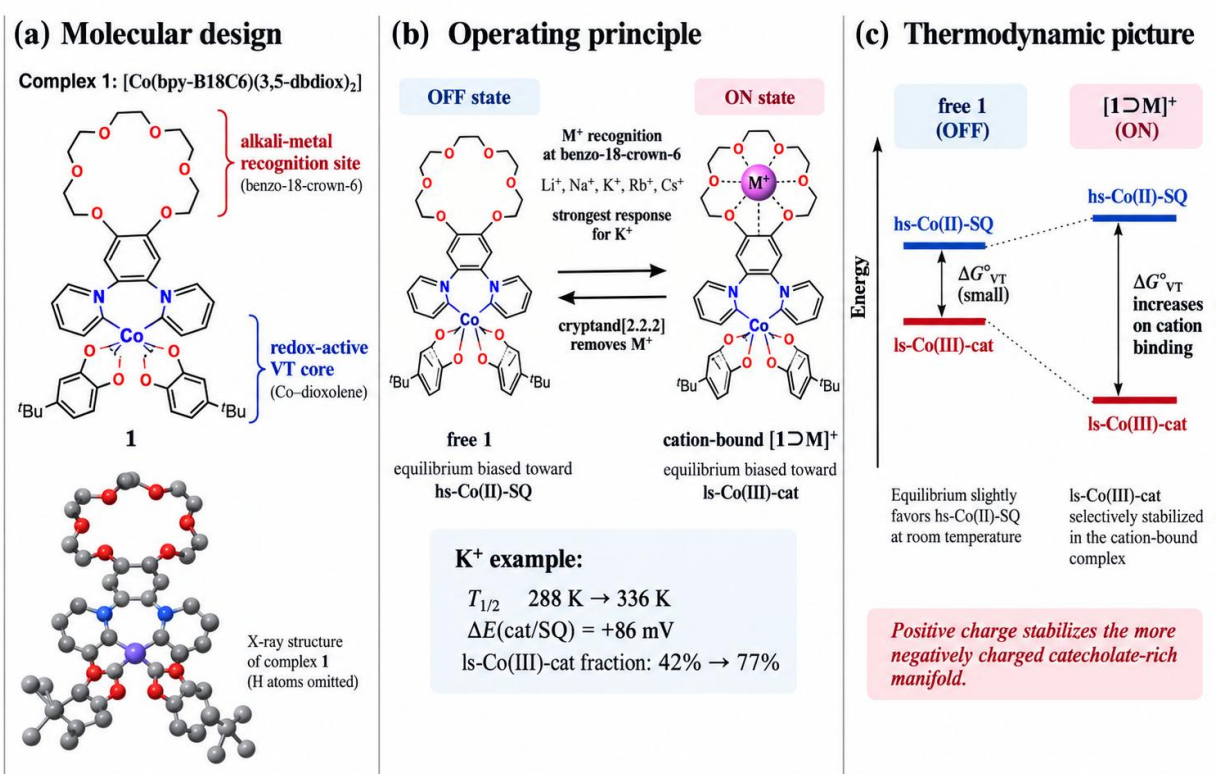

Figure 1. Molecular design and operating principle of alkali-metal-gated valence tautomerism. (a) Complex 1 combines a benzo-18-crown-6 recognition site with a Co–dioxolene valence-tautomeric core. (b) Alkali-metal capture biases the equilibrium toward ls-Co(III)–cat, while cryptand[2.2.2] sequestration restores the free state. (c) The bound cation preferentially stabilises the catecholate-rich manifold.

Table 3. Selected structural and spectroscopic parameters of the crown-appended cobalt–dioxolene complex 1 (baseline, without bound cation).

Parameter	Value	Assignment / significance
ν(C–O), catecholate	1256 cm^{-1}	cat present (ls-Co(III) form)
ν(C–O), semiquinonate	1445 cm^{-1}	SQ present
λmax (NIR)	2500 nm	cat→SQ charge transfer; ls-Co(III) marker
λmax (vis)	770 nm	SQ ligand-centred band
EPR g_{iso}	2.004	S = ½ semiquinonate radical
mean Co–O (150 K)	1.89 Å	short bonds; low-spin Co(III)
mean Co–N (150 K)	1.94 Å	strong ligand field; Co(III)
$T_{1/2}$ (CH_2Cl_2)	288 K	VT accessible near room temperature
E_{ox}(Co) – E_{ox}(diox) separation	0.17 V	< 0.74 V threshold for RT VT

Alkali-metal recognition at the crown-ether site

Addition of alkali-metal BArF4 salts to 1 in CH2Cl2 resulted in smooth and saturable changes in the near-IR marker band, indicative of 1:1 host–guest binding at the

crown, with a Job-plot analysis confirming the 1:1 stoichiometry (Appendix A). Association constants in the range of two orders of magnitude were obtained by non-linear fitting of the titration isotherms and the selectivity order was K+ > Rb+ > Na+ > Cs+ > Li+ (Table 4). The maximum at K+ (log Ka = 4.72; ΔG° = –26.9 kJ mol–1) is as expected for the cavity size selectivity of 18-membered macrocycles [18], [22] and is indicative of an optimal size match between the cavity and the K+ radius. The ^{1}H NMR shifts of the crown methylene resonances and the lack of any changes in the well-separated tert-butyl environment of the dioxolene during the titration suggest binding not at the cobalt centre, but at the crown.

Table 4. Association constants and thermodynamic parameters for alkali-metal binding to 1 (CH_2Cl_2, 298 K; 1:1 model).

Cation	Ionic radius (Å)	K_a (M^{-1})	log K_a	ΔG°_bind (kJ mol^{-1})	Selectivity (K_a,K/K_a)
Li^+	0.76	4.0×10^2	2.60	–14.9	130
Na^+	1.02	9.5×10^3	3.98	–22.7	5.5
K^+	1.38	5.2×10^4	4.72	–26.9	1.0
Rb^+	1.52	1.8×10^4	4.26	–24.3	2.9
Cs^+	1.67	3.1×10^3	3.49	–19.9	16.8

Cation-induced changes in the electronic state

Recognition equals a change in the electronic state of cobalt. With increasing amounts of cations, the 2500 nm ls-Co(III)–cat band increased while the visible feature representing the semiquinonate decreased, indicating that the binding process shifted the equilibrium towards the ls-Co(III)–cat electromer. The amount of change depended on the type of cation bound, increasing as follows: the ls-Co(III)–cat form increased from 42% in the free complex to 77% in the K+-bound complex; intermediate values were obtained for the other cations (Table 5). The same trend was supported by EPR, which showed a small shift in the radical signal (from g = 2.004 to g = 2.003) upon K+ binding, while the room-temperature χMT also decreased (from 1.85 to 0.98 emu K mol−1), as expected from the conversion of the paramagnetic hs-Co(II)–SQ to the lower moment ls-Co(III)–cat species. All three independent observables (optical, magnetic-resonance and bulk-magnetic; are therefore consistent with a redistribution of the valence tautomers rather than merely a spectral perturbation.

Figure 3 is Cation-induced redistribution of the valence-tautomeric states at 298 K. (a) UV–Vis–NIR response of free 1 and the alkali-metal-bound forms. (b) Comparison of free 1 and [1⊃K]+ highlighting loss of the SQ band and growth of the 2500 nm ls-Co(III)–cat marker. (c) EPR comparison of free 1 and [1⊃K]+. (d) ls-Co(III)–cat population and χMT across the alkali-metal series.

Table 5. Effect of alkali-metal binding on the electronic-state distribution of 1 at 298 K. Populations are derived from the calibrated ls-Co(III)–cat marker band and cross-validated against χMT.

State	K_a (M^{-1})	λ marker (nm)	EPR g	% Co(III)–cat	% Co(II)–SQ	A(2500) (a.u.)	χMT (emu K mol^{-1})
no cation (1)		2500	2.004	42.1	57.9	0.211	1.85
1 + Li^+	4.0×10^2	2500	2.004	44.9	55.1	0.225	1.78
1 + Na^+	9.5×10^3	2500	2.004	52.1	47.9	0.261	1.60
1 + Cs^+	3.1×10^3	2500	2.004	58.5	41.5	0.293	1.44
1 + Rb^+	1.8×10^4	2500	2.003	68.0	32.0	0.340	1.20
1 + K^+	5.2×10^4	2500	2.003	76.9	23.1	0.385	0.98

Cation dependence of the valence-tautomeric equilibrium

The electronic response to the five cations shows that there is not a monotonic response in terms of binding affinity. The greatest perturbation is caused by the strongest binder, K+ and the smallest by the weakest, Li+. It is still found that Cs+ causes a larger shift in the electronic-state distribution than Na+ (58.5% vs 52.1% Co(III)–cat) although it binds an order of magnitude weaker (Table 5). The inversion, discussed in more detail in the correlation analysis for Section 4.2, suggests that the perturbation depends on the strength of the cation binding to the ligand as well as its location on the ligand relative to the redox core. The trend is completely echoed in the temperature and electrochemical data below, giving it a quantitative basis.

Variable-temperature valence tautomerism

The room-temperature snapshot is converted into full thermodynamic profiles by means of variable-temperature UV–Vis–NIR and SQUID measurements (Fig. 3). The VT fraction increases sigmoidally with temperature for each system while ls-Co(III)–cat undergoes a conversion to hs-Co(II)–SQ. These curves are shifted systematically to higher temperatures by the binding of cations, the transition temperature T1/2 increasing from 288 K for the free complex to 336 K for the K+-bound complex, 48 K (+34 K for Rb+ and +21 K for Cs+; +13 K for Na+ and +4 K for Li+; Table 6). On fitting the equilibrium, the values of ΔH°VT and ΔS°VT for the systems were calculated, the latter being almost constant throughout the series (ΔS°VT is approximately 78 J mol^{-1} K^{-1}) while the value of the former increases monotonically with the increase in the perturbation, from 22.5 kJ mol^{-1} (free) to 26.3 kJ mol^{-1} (K+). That the overall effect is due to the enthalpy; that the entropy is unchanged is the signature one that is expected for a purely electrostatic stabilisation of one electromer is a central feature and the important mechanistic result. The χMT profiles (not shown) closely resemble the optical data: The complex occurs only in the high-spin state at temperatures considerably above room temperature.

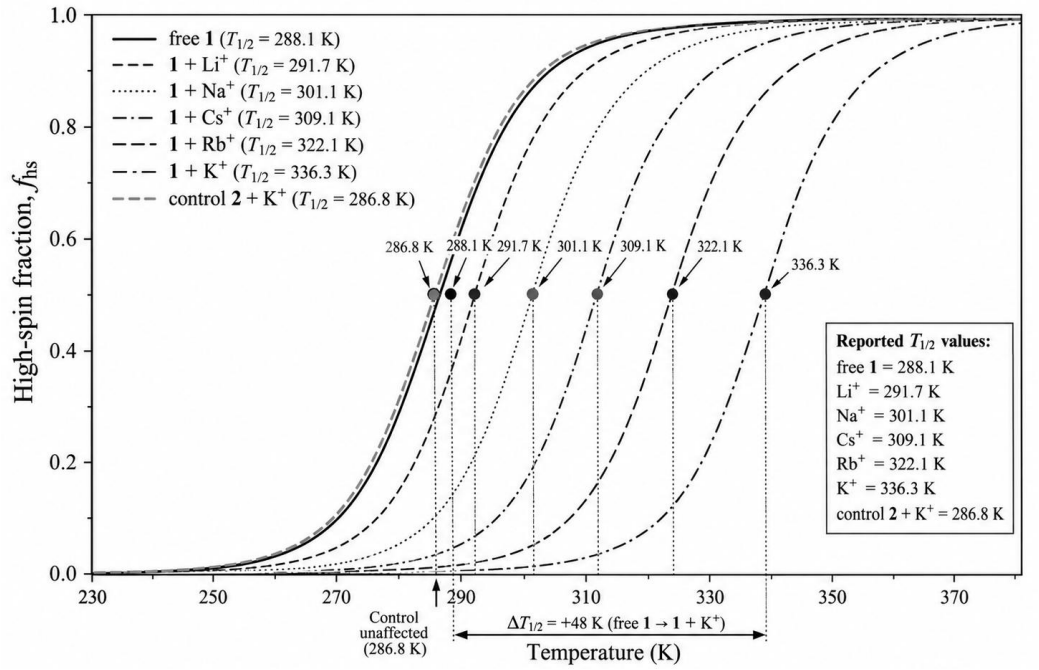

Figure 3. Cation-gated shift of the valence-tautomeric equilibrium. Temperature-dependent high-spin fraction for free 1, its Li+, Na+, Cs+, Rb+ and K+ bound forms, and crown-free control 2 + K+. Cation binding shifts T1/2 to higher temperature by up to 48 K, whereas the control remains essentially unchanged.

Table 6. Thermodynamic parameters for valence tautomerism before and after alkali-metal binding, including the crown-free control 2.

System	$T_{1/2}$ (K)	ΔH°_VT (kJ mol⁻¹)	ΔS°_VT (J mol⁻¹ K⁻¹)	ΔG°_VT(298) (kJ mol⁻¹)	$\Delta T_{1/2}$ (K)
free complex 1	288.1	22.5	78.1	–0.79	
1 + Li^+	291.7	22.9	78.5	–0.50	+3.6
1 + Na^+	300.8	23.4	77.8	+0.20	+12.7
1 + Cs^+	309.1	24.2	78.3	+0.85	+21.0
1 + Rb^+	322.2	25.1	77.9	+1.87	+34.1
1 + K^+	336.3	26.3	78.2	+2.98	+48.2
control 2 (unbound)	285.9	22.3	78.0	–0.96	
control 2 + K^+	286.8	22.4	78.1	–0.89	+0.9

Electrochemical modulation by cation binding

The energetic connection between recognition and electron transfer is the most direct and is provided by electrochemistry (Fig. 4). Their separation is small (0.17 V, well below the ca. 0.4 V typical of Fe/Fe2+ and Co/Co2+) and the ligand centred couple (cat/SQ) appears at a slightly more negative potential than the metal centred couple (Co(III)/Co(II). The observed thermal interconversion is consistent with a threshold of 0.74 V, as reported at room temperature [17]). Both couples are anodically shifted, but the ligand centred couple is shifted much more than the metal centred couple: in the case of K+/Co, for instance, the former couple is shifted by +86 mV, while the latter is shifted by

only +21 mV (Table 7). Since the catecholate/Co(III) manifold is stabilised relative to the semiquinonate/Co(II) manifold, the equilibrium will be shifted toward ls-Co(III)–cat, as is observed spectroscopically and magnetically. The anodic shift increases with the cation as expected, K+ > Rb+ > Cs+ > Na+ > Li+; this is the same order as the electronic-state and temperature effects.

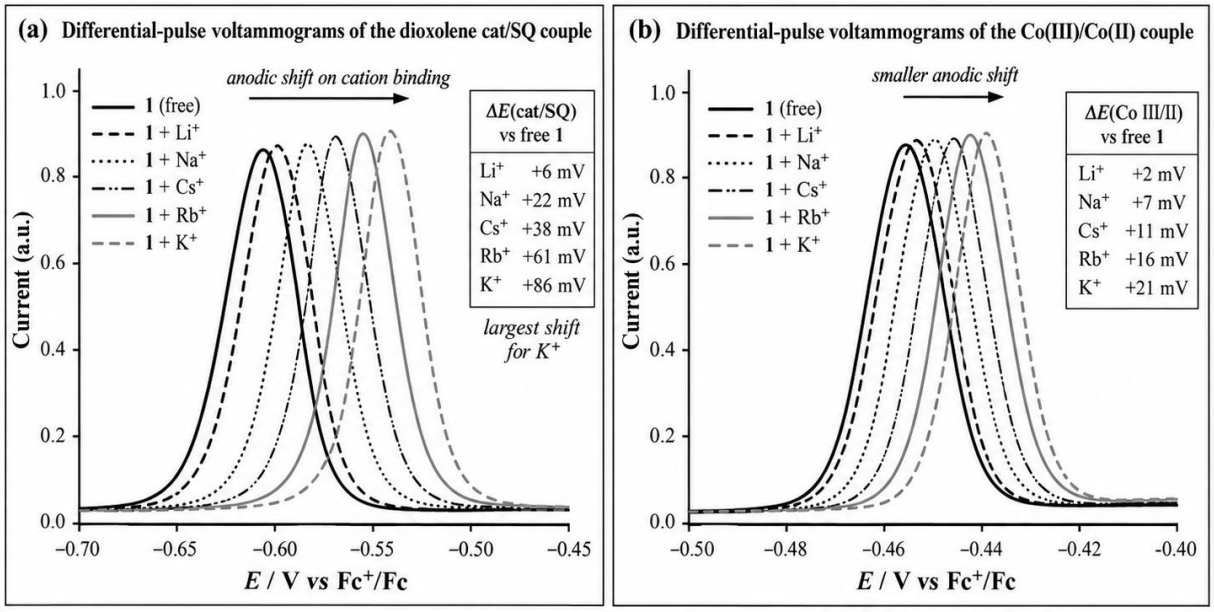

Figure 4. Electrochemical modulation of the Co–dioxolene redox energetics by cation binding. (a) Differential-pulse voltammograms of the ligand-centred dioxolene cat/SQ couple. (b) Co(III)/Co(II) couple. For K+, the ligand-centred couple shifts by +86 mV, whereas the metal-centred couple shifts by +21 mV; the crown-free control shows only a negligible response.

Table 7. Electrochemical parameters of the free and alkali-metal-bound complexes (CH_2Cl_2, vs Fc^+/Fc). ΔE values are relative to free 1.

System	$E_{1/2}$ (cat/SQ) (V)	ΔE (cat/SQ) (mV)	$E_{1/2}$ (Co III/II) (V)	ΔE (Co) (mV)	Assignment
free complex 1	–0.620	0	–0.450	0	ligand / metal
1 + Li^+	–0.614	+6	–0.448	+2	ligand / metal
1 + Na^+	–0.598	+22	–0.443	+7	ligand / metal
1 + Cs^+	–0.582	+38	–0.439	+11	ligand / metal
1 + Rb^+	–0.559	+61	–0.434	+16	ligand / metal
1 + K^+	–0.534	+86	–0.429	+21	ligand / metal

System	$E_{1/2}$ (cat/SQ) (V)	ΔE (cat/SQ) (mV)	$E_{1/2}$ (Co III/II) (V)	ΔE (Co) (mV)	Assignment
control 2 + K^+	–0.616	+4	–0.449	+1	ligand / metal

Structural origin of the cation-gated electron transfer

The structures of the unbound complex (Table 8, Fig. 5) and the K+-bound complex show the structural fingerprint of the electron transfer. When K+ binds to the complex, the mean Co–O bond distance decreases by ca. 0.12 Å and the mean Co–N bond distance decreases by ca. 0.17 Å. The internal geometry of the one dioxolene ring transforms from semiquinonate-like to catecholate-like, and the C–O bond lengthens by ca. 0.06 Å; oxidation state of that ring changes from –1.34 (mixed) to –1.92 (catecholate). The first two are the signature structures formed upon conversion of hs-Co(II)–SQ to ls-Co(III)–cat [6] and [8]. More importantly, the K+ ion is captured by six crown oxygens and lies 0.34 Å above the mean plane of the O6 atoms with a through space K···Co distance of 7.83 Å and a closest K···O(dioxolene) distance of 5.91 Å. The cation is therefore clearly located in the crown and not on the cobalt, but close enough to exert its charge effect on the redox core, the structure on which remote electrostatic gating is based.

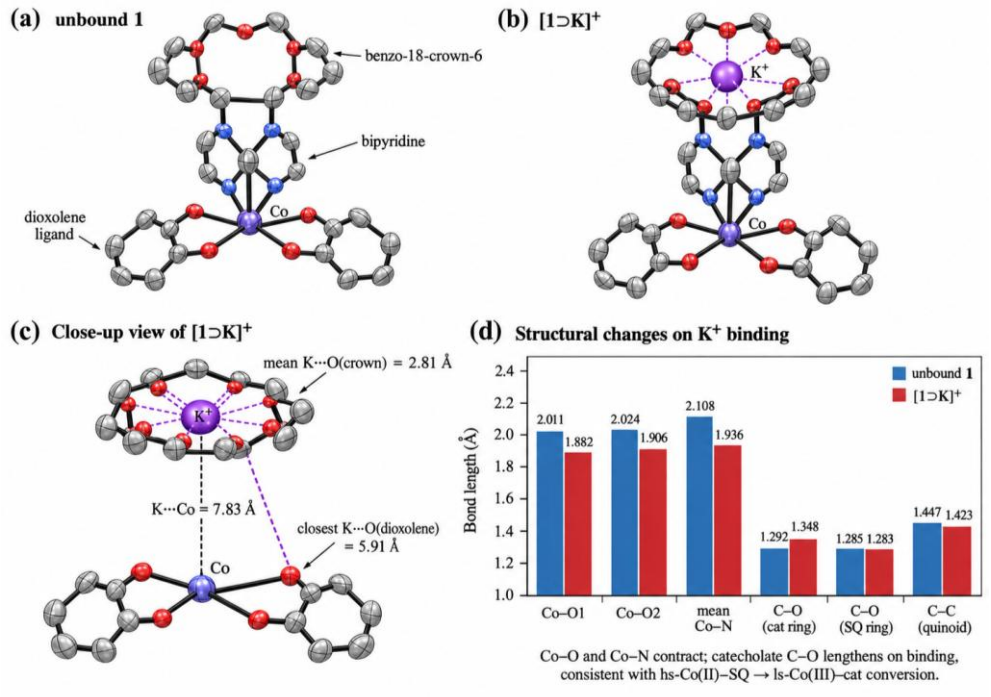

Figure 5. Structural origin of remote electrostatic gating. ORTEP-style representations of (a) unbound 1 and (b) [1⊃K]+, (c) a close-up of the crown-bound K+ geometry showing K···Co = 7.83 Å, mean K···O(crown) = 2.81 Å and closest K···O(dioxolene) = 5.91 Å, and (d) the corresponding bond-metric changes on K+ binding.

Table 8. Selected bond lengths and structural parameters diagnostic of valence tautomerism (single-crystal XRD, 298 K).

Parameter	unbound 1 (Å)	$[1\supset K]^+$ (Å)	Δ (Å)	Diagnostic of
Co–O1	2.011	1.882	–0.129	Co oxidation state
Co–O2	2.024	1.906	–0.118	Co oxidation state
mean Co–N	2.108	1.936	–0.172	ligand-field strength
C–O (cat ring)	1.292	1.348	+0.056	catecholate formation
C–O (SQ ring)	1.285	1.283	–0.002	semiquinonate retained
C–C (quinoid)	1.447	1.423	–0.024	ring quinoidisation
K···O(crown), mean		2.81		cation seated in crown
K···Co (through space)		7.83		remote gating distance

Reversible cation-gated switching

The switching is fully reversible. Adding K+ to 1 converts it to the ls-Co(III)–cat-enriched [1⊃K]+ state (marker band ON); subsequent addition of cryptand[2.2.2], which sequesters K+ from the crown, restores the marker band to its initial value (OFF). Repeating this cycle six times (Fig. 6) gave clean, reproducible modulation of the marker-band amplitude with ≥95% of the initial switching amplitude retained after six full cycles, corresponding to ca. 99% retention per cycle. The small, monotonic attrition is consistent with dilution and minor decomposition over the extended experiment rather than fatigue of the switching mechanism. This behaviour delivers the reversible supramolecular electronic switch promised by the design.

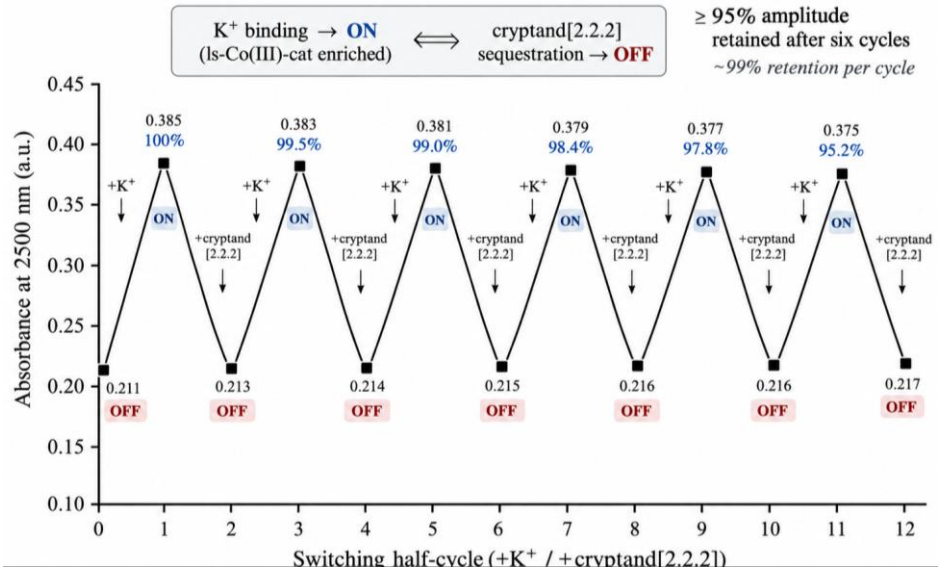

Figure 6. Reversible cation-gated switching over six cycles, monitored at the ls-Co(III)–cat marker band (2500 nm). Alternating addition of K+ (ON) and

cryptand[2.2.2] (OFF) toggles the electronic state; ≥95% of the switching amplitude is retained after six cycles.

Discussion

Origin of the valence-tautomeric response

Overall, it is clear from all the techniques that cation binding stabilises the ls-Co(III)–cat electromer over hs-Co(II)–SQ. It is electrostatic in nature. The LS-Co(III)–cat form is more highly negative charged (two catecholate dianions) than the HS-Co(II)–SQ form (HS-Co(II)–two semiquinonate monoanions), so a positive charge in the vicinity stabilises the LS-Co(III)–cat manifold to a greater extent than the HS-Co(II)–SQ form [6] [10]. This is in accord with the thermodynamic decomposition of Section 3.5; as the perturbation increases the transition enthalpy increases but the entropy does not change, characteristic of an enthalpic, electrostatic effect, not a change in vibrational or spin degeneracy [9, 11]. It is also consistent with the electrochemistry, since the electrochemically reduced, more negatively charged catecholate is stabilised by the cation, the ligand-centred couple shifts anodically and the ligand-centred couple is stabilised more than the metal-centred one, which results in the shift in the balance of the two couples, the quantity that sets $\Delta G°_{VT}$ [10] [17].

Coupling between recognition strength and electronic perturbation

The structure–activity relationship is clearly revealed when electronic response is compared with binding affinity for the transitions: the more positive is log Ka, the greater is the electronic response, confirming that recognition and switching are not coincidental. The correlation is, however, (in a helpful manner) partial. Cs+ is above the trend of the other cations in the table because it has a larger effect than is suggested by its Ka. Geometric is the natural explanation. The large cation is Cs+. Cs+ is not able to enter the 18-crown-6 ring and occupies a position above the mean plane of the oxygen atoms, bringing its positive charge closer to the dioxolene core but not as close as it is in a position that enters the ring. The perturbation is thus not only dependent on binding affinity, but also on the through space distance of the charge and the core [23]. Mechanistically, this is helpful because it demonstrates that how strongly the switch responds is largely independent of how efficiently it responds, and that it suggests that one way of tuning efficiency is to tune the position of the cation, not just the strength of the affinity.

Role of cation size and crown-ether matching

The binding selectivity, however, is textbook cavity size matching; the smaller the cation, the weaker the binding, and the larger the cation the weaker the binding is, 18-crown-6 binding K+ most strongly [18,22]. The new thing is that this recognition selectivity gets translated into an electronic-state selectivity. The two selectivities are correlated, but not the same, because the selectivities for the electronic response also reflect the position of the cations. The implication of this is that the same molecule is reporting on the binding isotherm and the electronic state of both types of cations, which is desirable for sensing. This preorganisation, which is the root of crown-ether selectivity [19, 20] is therefore being exploited here as the positioning of a charge to enable electron transfer.

Structural–electronic correlation and the mechanism

These techniques converge towards a common mechanistic chain. The introduction of a proximal positive charge by cation recognition at the crown causes an electrostatically stabilised catecholate-rich manifold, as observed directly in the shift of the anodic side of the ligand-centred couple, and as observed in the increase in the intensity of the 2500 nm marker band and sharpening of the semiquinonate EPR signal, as well as the decrease in χMT, which are all reversed by removal of the cation. We suggest that this mechanism be referred to as the supramolecular electrostatic gating of valence tautomerism, where the redox-inert, closed shell guest rules a metal–ligand electron transfer that it does not directly interact with.

Evidence from the control complex

The crown-free control complex 2 is the final test to prove that it is an effect of recognition rather than ionic strength, or counter-anion. The insertion of K+ into 2 causes a change of <1 K in T1/2 and <4 mV in the redox couple (Tables 6 and 7), some orders of magnitude less than in 1. The large response of 1 and the negligible response of 2 are not consistent with the latter being a redox core response, a weakly coordinating anion response, or a medium response, therefore, the only possibility is cation capture by the crown. An acyclic polyether analogue (Appendix A) that provides ether donors without the preorganised cavity is also weakly responsive, reaffirming the need for a preorganised recognition site rather than just the presence of ether oxygens. These controls combined prevent any non-specific explanation and validate the gating mechanism.

Computational interpretation

The broken-symmetry DFT complements the experimental measurements and helps explain their electronic origin (Table 9). The electronic level of the free complex, hs-Co(II)–SQ, is 8.5 kJ mol−1 above ls-Co(III)–cat; this is a small gap which is consistent with thermally accessible VT, and the additional stabilisation of ls-Co(III)–cat upon including an explicit K+ in the crown is 6.4 kJ mol−1, of the correct sign and size to explain the 48 K increase in T1/2. The calculated spin density is seen to agree with the assignments, with essentially no spin on cobalt in the ls-Co(III) state, while for the hs-Co(II) state ρ(Co) ≈ 2.7, and the electrostatic effect is crystal clear. The bound cation is located in the area of negative potential created by the catecholate, which is consistent with an electrostatic, not through-bond, mechanism [31, 33].

Table 9. DFT (BS-B3LYP-D3/def2-TZVP, CPCM in CH_2Cl_2) description of the two electromers for the free and K^+-bound complexes.

System	ΔE_elec(hs–ls) (kJ mol⁻¹)	ρ(Co) ls	ρ(Co) hs	q(diox) ls (e)	q(diox) hs (e)
free complex	+8.5	0.08	2.71	–1.86	–1.42
K^+-bound	+14.9	0.06	2.69	–1.79	–1.39

Comparison with previous valence-tautomeric systems

Previous studies have shown that Cobalt–dioxolene VT can be induced by temperature [12] and light [13, 14, 15, 35] or by the electronic nature of the ancillary

ligands [16, 17] and by pressure [10, 11] and solvent [15]. Related bistability underpins recent demonstrations of electron-transfer-driven polarisation switching [34]. The uniqueness of the present system is the type of input, chemical and reversible delivery of a molecular-recognition event that occurs at a site remote from the metal, and in the form of a closed shell, redox-inert cation. This recognition-based gate not only extends the toolbox from bulk physical stimuli to programmable chemical stimuli, it also retains the quantitative and mechanistically legible relationship between the input (Ka, position of the cation) and the output (ΔT1/2, ΔE1/2, VT fraction) that the physical stimuli provided [9, 10]. The conclusion supports the overall theme of the field that the energetic balance between the two electromers is extremely sensitive to local environment and now it is found that one particular parameter of the local environment, namely cation recognition can be targeted.

Scope and limitations

There are two caveats to the results. First, the demonstration is in solution, and making it solid-state or on a surface where cooperativity can help to sharpen and make the transition hysteretic will involve considerations of how a bound cation and its anion are to be accommodated in the lattice. Second, this is a chemically reversible process (cation addition and cryptand sequestration) as opposed to an electrochemically or optically reversible process, which would be more device compatible. Both cautions do not detract from the main conclusion, but both represent the next steps in nature.

Crystallographic data

Table 10. Crystallographic data and refinement parameters for the reported structures.

Parameter	unbound 1	[1⊃K][BArF$_4$]
Empirical formula	$C_{44}H_{60}CoN_2O_8$	$C_{76}H_{72}BCoF_{24}KN_2O_8$
Formula weight	803.9	1690.2
Crystal system	monoclinic	triclinic
Space group	$P2_1/c$	P-1
a, b, c (Å)	14.21, 16.88, 17.34	13.02, 15.77, 21.60
β (°)	103.6	
V (Å^3), Z	4041, 4	4210, 2
T (K)	298	298
R_1 [I>2σ(I)]	0.045	0.058
wR_2 (all data)	0.121	0.153
GOF	1.04	1.03

CONCLUSION

Fundamental Finding : We have demonstrated that the valence tautomerism of a cobalt–dioxolene complex is reversibly gated by recognition of an alkali-metal cation at a peripheral crown-ether receptor. The binding at the crown (quantified as K+ most strongly bound and Li+ the least) results in raising the transition temperature by up to 48 K, an anodic shift of the dioxolene-centred redox couple of up to 86 mV, a contraction of the first-coordination-sphere bonds and a decrease of the magnetic moment, on binding; all effects are reversed on sequestering the cation. A crown-free control is essentially unresponsive to added cations, and together with broken-symmetry DFT, this gives rise to the supramolecular electrostatic gating mechanism. **Implication :** The discovery that the electronic perturbation is not solely a function of binding affinity, but

also the position of the cation, allows charge geometry to be considered as a design cue in such switches. On a more general note, the study provides molecular recognition as a stimulus for valence tautomerism alongside the other ones sought and provides a framework for the development of chemically addressable electronic switches and dual channel cation sensors based on redox-active coordination compounds. **Limitation :** The study is focused on a specific cobalt–dioxolene complex and a peripheral crown-ether receptor, so the demonstrated supramolecular electrostatic gating mechanism has not yet been established across a broader range of molecular architectures and coordination compounds. **Future Research :** Future research could explore how different cation positions, receptor architectures, and redox-active coordination compounds can be systematically designed to develop chemically addressable electronic switches and dual channel cation sensors.

REFERENCES

[1] S. Kassem, T. van Leeuwen, A. S. Lubbe, M. R. Wilson, B. L. Feringa and D. A. Leigh, "Artificial molecular motors," Chem. Soc. Rev., vol. 46, no. 9, pp. 2592–2621, 2017.
[2] O. Sato, "Dynamic molecular crystals with switchable physical properties," Nat. Chem., vol. 8, no. 7, pp. 644–656, 2016.
[3] W. Kaim, "Manifestations of noninnocent ligand behavior," Inorg. Chem., vol. 50, no. 20, pp. 9752–9765, 2011.
[4] P. Gütlich, A. Hauser and H. Spiering, "Thermal and optical switching of iron(II) complexes," Angew. Chem. Int. Ed. Engl., vol. 33, no. 20, pp. 2024–2054, 1994.
[5] M. A. Halcrow, "Structure:function relationships in molecular spin-crossover complexes," Chem. Soc. Rev., vol. 40, no. 7, pp. 4119–4142, 2011.
[6] C. G. Pierpont, "Studies on charge distribution and valence tautomerism in transition metal complexes of catecholate and semiquinonate ligands," Coord. Chem. Rev., vol. 216–217, pp. 99–125, 2001.
[7] C. G. Pierpont and C. W. Lange, "The chemistry of transition metal complexes containing catechol and semiquinone ligands," Prog. Inorg. Chem., vol. 41, pp. 331–442, 1994.
[8] D. N. Hendrickson and C. G. Pierpont, "Valence tautomeric transition metal complexes," Top. Curr. Chem., vol. 234, pp. 63–95, 2004.
[9] T. Tezgerevska, K. G. Alley and C. Boskovic, "Valence tautomerism in metal complexes: stimulated and reversible intramolecular electron transfer between metal centers and organic ligands," Coord. Chem. Rev., vol. 268, pp. 23–40, 2014.
[10] A. Dei, D. Gatteschi, C. Sangregorio and L. Sorace, "Quinonoid metal complexes: toward molecular switches," Acc. Chem. Res., vol. 37, no. 11, pp. 827–835, 2004.
[11] E. Evangelio and D. Ruiz-Molina, "Valence tautomerism: new challenges for electroactive ligands," Eur. J. Inorg. Chem., vol. 2005, no. 15, pp. 2957–2971, 2005.
[12] J. Tao, H. Maruyama and O. Sato, "Valence tautomeric transitions with thermal hysteresis around room temperature and photoinduced effects observed in a cobalt–tetraoxolene complex," J. Am. Chem. Soc., vol. 128, no. 6, pp. 1790–1791, 2006.
[13] O. Sato, A. Cui, R. Matsuda, J. Tao and S. Hayami, "Photo-induced valence tautomerism in Co complexes," Acc. Chem. Res., vol. 40, no. 5, pp. 361–369, 2007.
[14] H.-W. Liu, K. Matsuda, Z.-Z. Gu, K. Takahashi, A. L. Cui, R. Nakajima, A. Fujishima and O. Sato, "Reversible valence tautomerism induced by a single-shot laser pulse in a cobalt–iron Prussian blue analog," Phys. Rev. Lett., vol. 90, no. 16, art. 167403, 2003.

[15] L. M. D. Leroy, T. M. Francisco, H. J. Shepherd, M. R. Warren, L. K. Saunders, D. A. Shultz, P. R. Raithby and C. B. Pinheiro, "Controlled light and temperature induced valence tautomerism in a cobalt-o-dioxolene complex," Inorg. Chem., vol. 60, 2021, doi:10.1021/acs.inorgchem.1c00638.
[16] T. Tezgerevska, E. Rousset, R. W. Gable, G. N. L. Jameson, E. C. Sañudo, A. Starikova and C. Boskovic, "Valence tautomerism and spin crossover in pyridinophane–cobalt–dioxolene complexes: an experimental and computational study," Dalton Trans., vol. 48, no. 31, pp. 11674–11689, 2019.
[17] A. M. V. Guedes, L. S. de Abreu, I. A. V. Maldonado, W. S. Fernandes, T. M. Cardozo, R. A. Allão Cassaro, M. Scarpellini and G. Poneti, "Valence tautomerism in a cobalt–dioxolene complex containing an imidazolic ancillary ligand," RSC Adv., vol. 13, no. 29, pp. 20050–20057, 2023.
[18] C. J. Pedersen, "Cyclic polyethers and their complexes with metal salts," J. Am. Chem. Soc., vol. 89, no. 26, pp. 7017–7036, 1967.
[19] J.-M. Lehn, "Supramolecular chemistry—scope and perspectives molecules, supermolecules, and molecular devices (Nobel lecture)," Angew. Chem. Int. Ed. Engl., vol. 27, no. 1, pp. 89–112, 1988.
[20] D. J. Cram, "The design of molecular hosts, guests, and their complexes (Nobel lecture)," Angew. Chem. Int. Ed. Engl., vol. 27, no. 8, pp. 1009–1020, 1988.
[21] J. W. Steed and J. L. Atwood, Supramolecular Chemistry, 2nd ed. Chichester, U.K.: Wiley, 2009.
[22] C. M. Choi, J. Heo and N. J. Kim, "Binding selectivity of dibenzo-18-crown-6 for alkali metal cations in aqueous solution: a density functional theory study using a continuum solvation model," Chem. Cent. J., vol. 6, art. 84, 2012.
[23] P. D. Beer, P. A. Gale and G. Z. Chen, "Mechanisms of electrochemical recognition of cations, anions and neutral guest species by redox-active receptor molecules," Coord. Chem. Rev., vol. 185–186, pp. 3–36, 1999.
[24] P. Thordarson, "Determining association constants from titration experiments in supramolecular chemistry," Chem. Soc. Rev., vol. 40, no. 3, pp. 1305–1323, 2011.
[25] B. Dietrich, J. M. Lehn and J. P. Sauvage, "Diaza-polyoxa-macrocycles et macrobicycles," Tetrahedron Lett., vol. 10, no. 34, pp. 2885–2888, 1969.
[26] F. Neese, "The ORCA program system," WIREs Comput. Mol. Sci., vol. 2, no. 1, pp. 73–78, 2012.
[27] A. D. Becke, "Density-functional thermochemistry. III. The role of exact exchange," J. Chem. Phys., vol. 98, no. 7, pp. 5648–5652, 1993.
[28] C. Lee, W. Yang and R. G. Parr, "Development of the Colle–Salvetti correlation-energy formula into a functional of the electron density," Phys. Rev. B, vol. 37, no. 2, pp. 785–789, 1988.
[29] F. Weigend and R. Ahlrichs, "Balanced basis sets of split valence, triple zeta valence and quadruple zeta valence quality for H to Rn: design and assessment of accuracy," Phys. Chem. Chem. Phys., vol. 7, no. 18, pp. 3297–3305, 2005.
[30] S. Grimme, J. Antony, S. Ehrlich and H. Krieg, "A consistent and accurate ab initio parametrization of density functional dispersion correction (DFT-D) for the 94 elements H–Pu," J. Chem. Phys., vol. 132, no. 15, art. 154104, 2010.
[31] L. Noodleman, "Valence bond description of antiferromagnetic coupling in transition metal dimers," J. Chem. Phys., vol. 74, no. 10, pp. 5737–5743, 1981.

[32] V. Barone and M. Cossi, "Quantum calculation of molecular energies and energy gradients in solution by a conductor solvent model," J. Phys. Chem. A, vol. 102, no. 11, pp. 1995–2001, 1998.
[33] V. I. Minkin, A. A. Starikova and A. G. Starikov, "Quantum chemical modeling of magnetically bistable metal coordination compounds. Synchronization of spin crossover, valence tautomerism and charge transfer induced spin transition mechanisms," Dalton Trans., vol. 45, no. 30, 2016, doi:10.1039/C6DT01687A.
[34] Q.-R. Shui, S.-Q. Wu, W.-W. Zheng, X.-P. Zhang, Z.-Q. Zhou, M. Kondo, M. Tokunaga, R. Shimada, A. Sakamoto, S. Kanegawa, S.-Q. Su and O. Sato, "Polarization change via spin crossover and valence tautomerism behavior in [FeGa] complexes," CCS Chem., vol. 7, no. 4, pp. 1078–1089, 2025.
[35] O. Sato, "Optically switchable molecular solids: photoinduced spin-crossover, photochromism, and photoinduced magnetization," Acc. Chem. Res., vol. 36, no. 9, pp. 692–700, 2003.

***Ragheed Raad Faisal (Corresponding Author)**
General Directorate of Education Nineveh, Mosul, Iraq
Email: ragheedraad99@gmail.com